Zhang et al., http://www.jgp.org/cgi/content/full/jgp.201311084/DC1

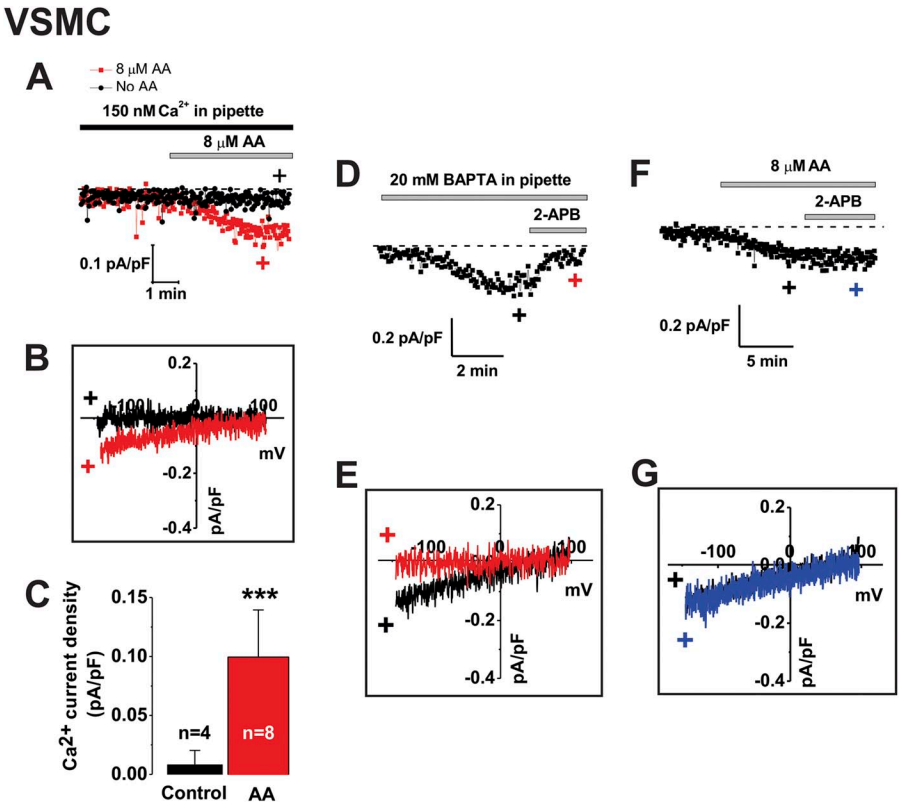

Figure S1. AA activates Ca^{2+} currents in VSMCs. Representative time courses (A) of whole-cell inward currents sampled at −100 mV showing that AA activates an inward Ca^{2+} current in VSMCs bathed in 20 mM of extracellular Ca^{2+}. 50 μM 2-APB, a CRAC channel blocker, did not block AA-activated currents (F). However, 2-APB at the same concentration abolished CRAC currents activated by store depletion through dialysis of 20 mM BAPTA through the patch pipette (D). Representative I-V curves are shown in B, E, and G, respectively. Statistical analysis on current densities of AA-activated currents and control (without AA) is shown in C. The sample size, mean/range, and p-values for statistical comparisons for this figure and all subsequent supplemental figures are reported in Table S3.

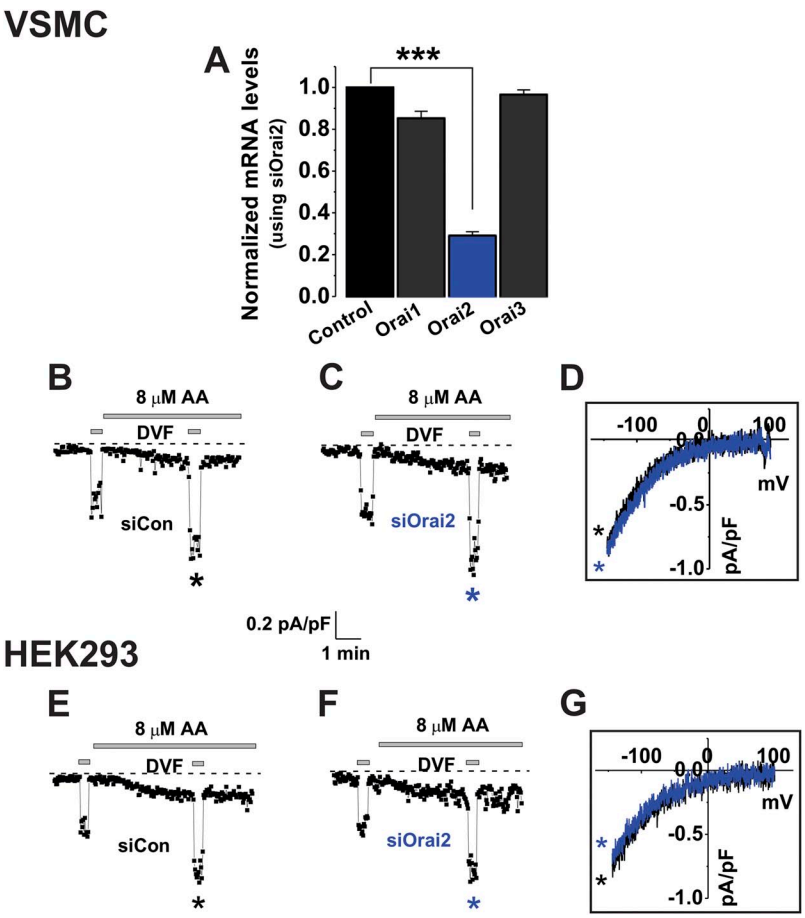

Figure S2. Orai2 knockdown has no effect on AA-activated currents in VSMCs and HEK293 cells. Quantitative RT-PCR shows Orai2 mRNA knockdown upon transfection of VSMCs with specific siRNA against Orai2 (A; no effect was observed on Orai1 or Orai3 expression). Statistical analyses on data are from three independent transfections, each performed in triplicates. (B–G) Orai2 knockdown (C, VSMCs; F, HEK293 cells) has no effect on AA-activated currents as compared with control siRNA (B, VSMCs; E, HEK293 cells). Representative Na^+ I-V relationships for AA-activated currents in VSMCs and HEK293 cells are shown in D and G, respectively. Statistical analyses on these data are shown in Fig. 2 (E and I) in the main text.

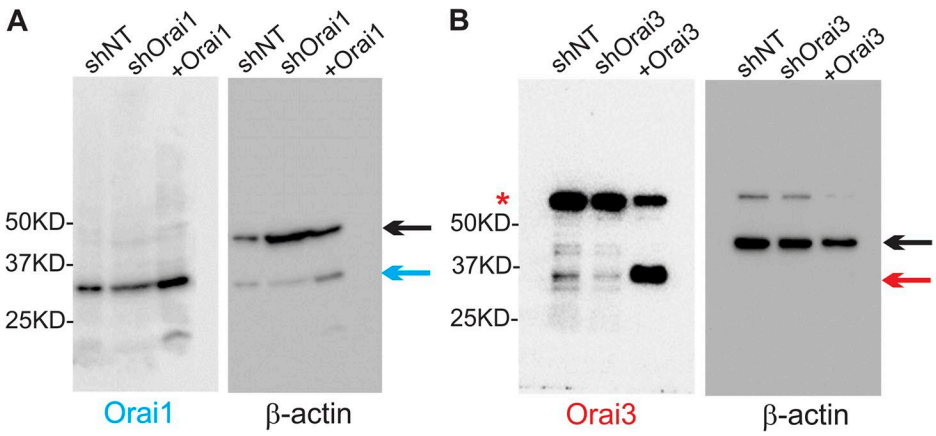

Figure S3. Validation of Orai1 and Orai3 antibodies by Western blotting. (A) Western blotting using anti-Orai1 antibody on HEK293 cells transfected with either control shRNA, Orai1 shRNA, or a plasmid encoding Orai1 cDNA; the β-actin loading control was performed on the stripped and reprobed membrane. Orai1 and β-actin positions are indicated by blue and black arrows, respectively. (B) Western blotting using anti-Orai3 antibody on HEK293 cells transfected with control shRNA, Orai3 shRNA, or a plasmid encoding Orai3 cDNA; the β-actin loading control is also shown. Orai3 and β-actin positions are indicated by red and black arrows, respectively. The band labeled with the red asterisk is a nonspecific band.

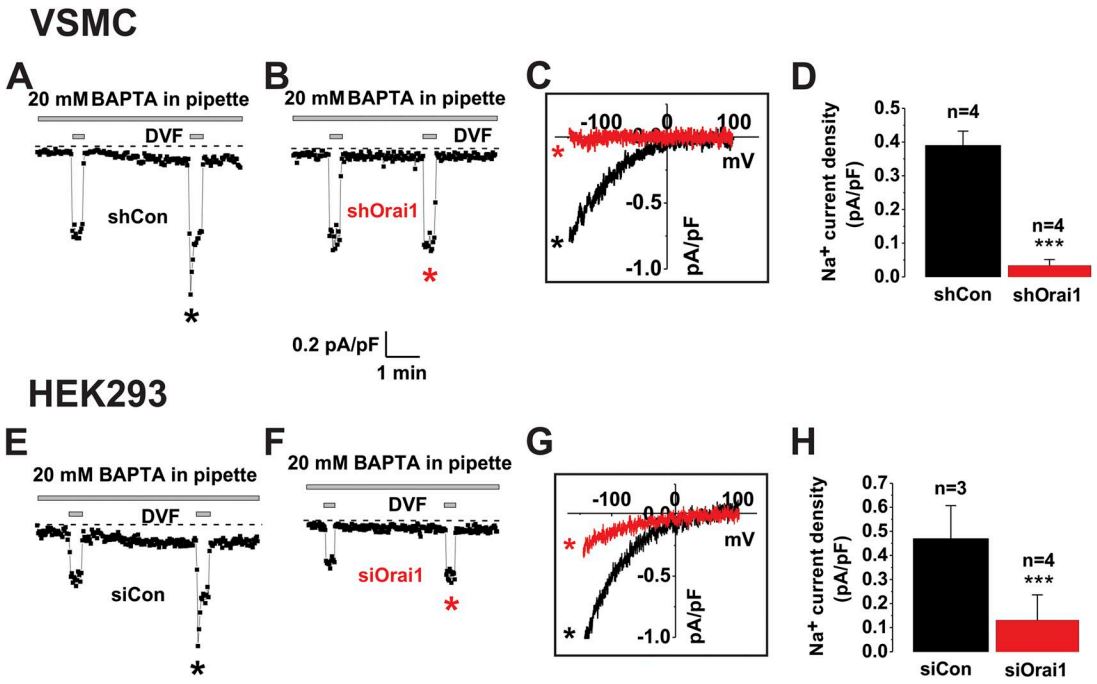

Figure S4. Orai1 knockdown abrogates store depletion–activated CRAC currents in VSMCs and HEK293 cells. Whole-cell electrophysiological recordings in VSMCs infected with lentiviruses encoding shRNA against Orai1 (shOrai1) or shControl, a nontargeting control. Respective time course of whole-cell inward currents sampled at −100 mV shows that Orai1 knockdown abrogated Na^+/Ca^{2+} CRAC currents (B) as compared with control (A). In HEK293 cells, Orai1 knockdown was achieved by transfection of siRNA targeting Orai1 (siOrai1). siOrai1 significantly inhibited Na^+/Ca^{2+} CRAC currents (F) as compared with siControl (E). Representative Na^+ I-V relationships of CRAC currents in VSMCs (C) and HEK293 cells (G) are shown. Statistical analysis on these data is shown in D and H, respectively.

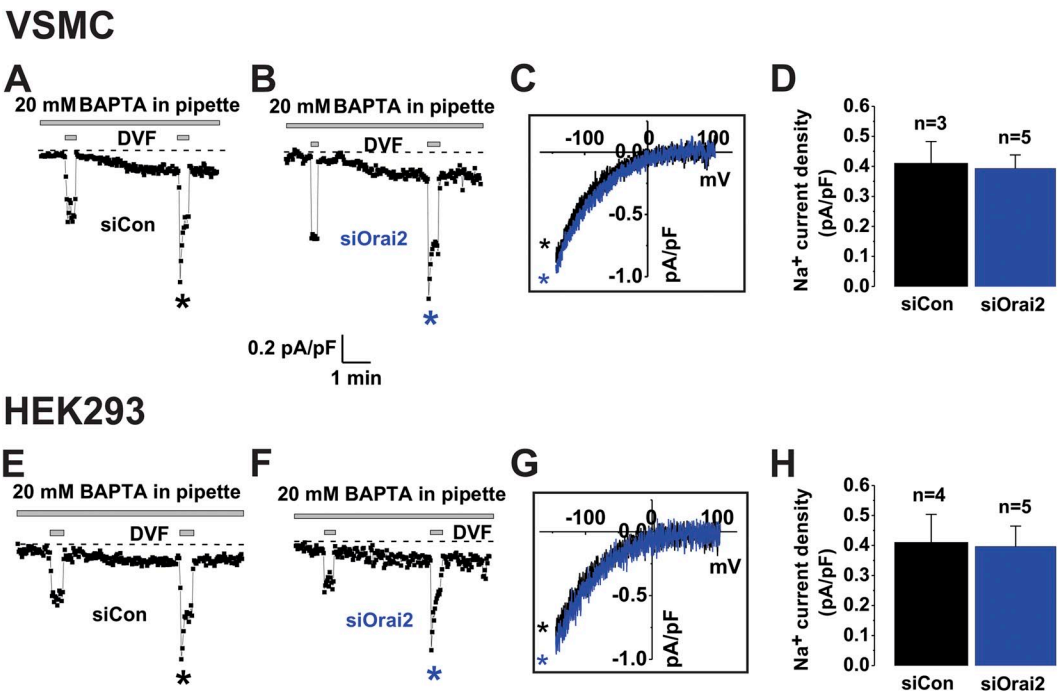

Figure S5. Orai2 knockdown had no effect on CRAC current in both VSMCs and HEK293 cells. Whole-cell electrophysiological recording in VSMCs (A–D) or HEK293 cells (E–H) transfected with specific siRNA against Orai2 (siOrai2) or siControl, a nontargeting siRNA control. Respective time courses of whole-cell CRAC currents sampled at −100 mV show that Orai2 knockdown had no effect with Na^+/Ca^{2+} CRAC currents (B, VSMCs; F, HEK293 cells) as compared with control (A, VSMCs; E, HEK293 cells). Representative Na^+ I-V relationships of CRAC currents in VSMCs and HEK293 cells are shown in C and G, respectively. Statistical analysis on these data is shown in D and H, respectively.

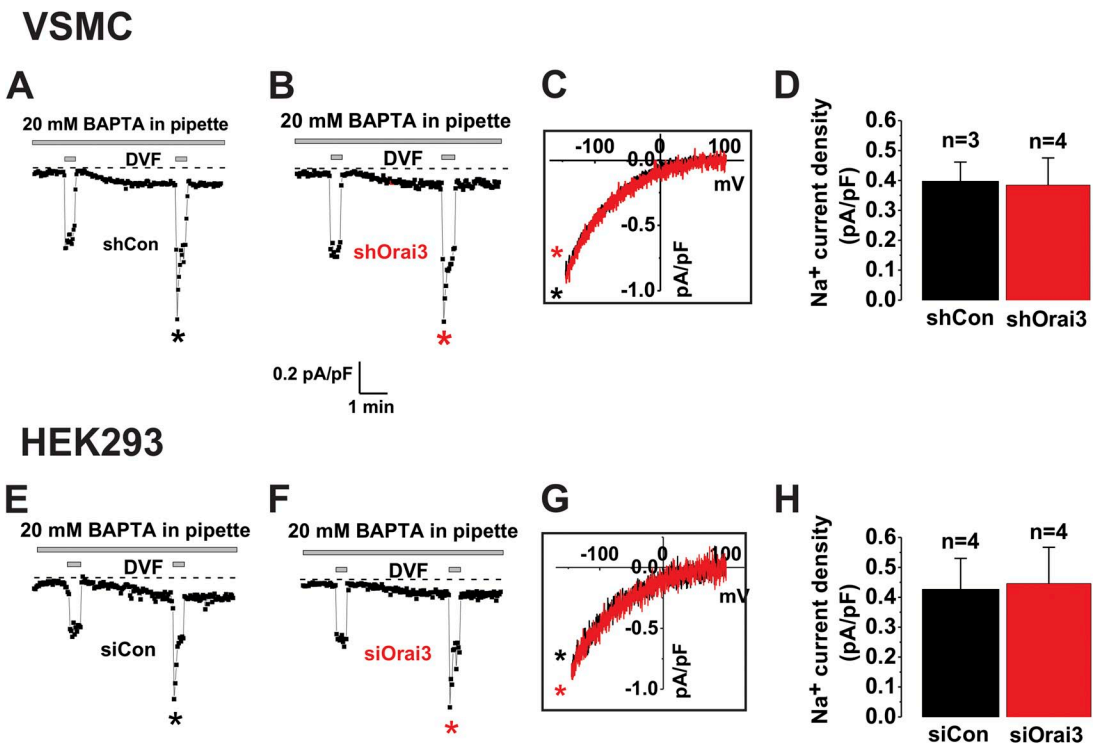

Figure S6. Orai3 knockdown had no effect on CRAC current in both VSMCs and HEK293 cells. Whole-cell electrophysiological recordings in VSMCs infected with lentiviruses encoding shRNA against Orai3 (shOrai3) or shControl, a nontargeting control. Respective time courses of whole-cell inward currents sampled at −100 mV show that Orai3 knockdown had no effect with Na^+/Ca^{2+} CRAC currents (B) as compared with control (A). In HEK293 cells, Orai3 knockdown was achieved by transfection of siRNA targeting Orai3 (siOrai3). siOrai3 had no effect with Na^+/Ca^{2+} CRAC currents (F) as compared with control siRNA (E). Representative Na^+ I-V relationships of CRAC currents in VSMCs and HEK293 cells are shown in C and G, respectively. Statistical analysis on these data is shown in D and H, respectively.

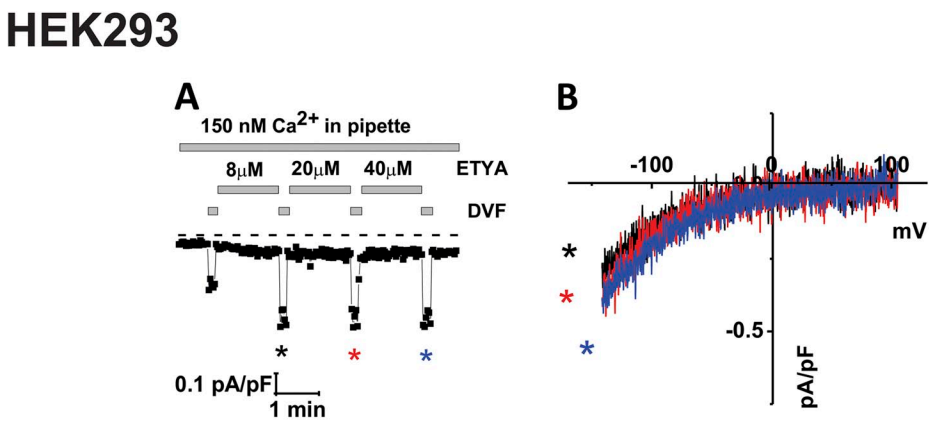

Figure S7. High concentrations of ETYA do not cause further increase in AA-activated current density in HEK293 cells. Whole-cell patch-clamp electrophysiological recording on HEK293 cells. 8 μM ETYA and subsequent addition of higher concentration of ETYA (20 and 40 μM) did not cause further increase in AA-activated current density (A). Representative I-V curves taken where indicated by colored asterisks are shown in B.

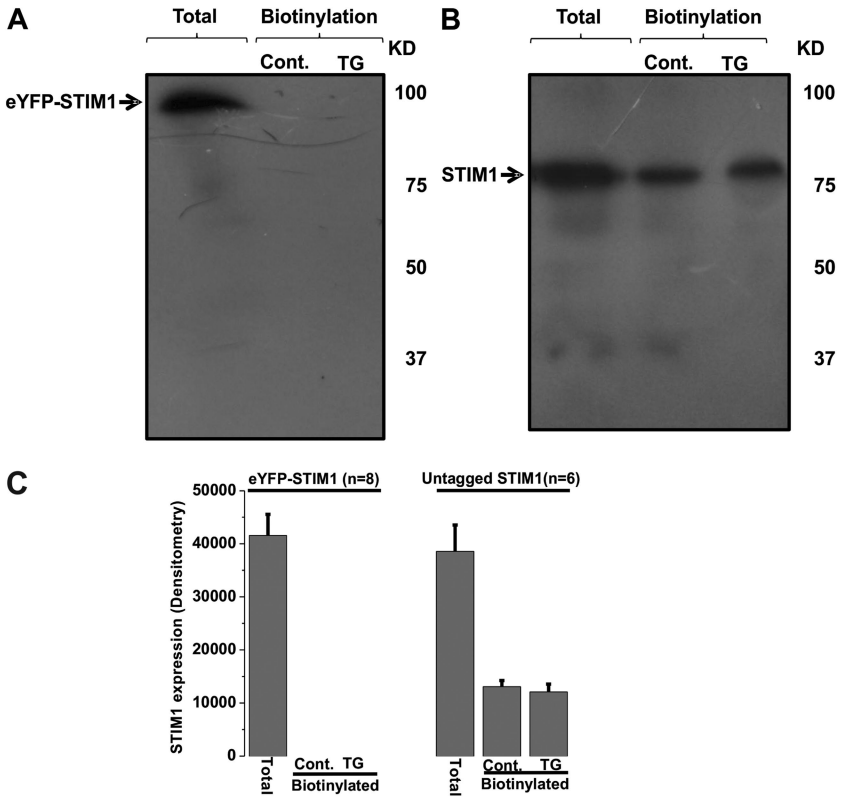

Figure S8. Cell surface expression of eYFP-STIM and untagged WT STIM1. HEK293 cells expressing either eYFP-tagged on N terminus (A) or untagged WT STIM1 (B) were either left untreated (lane 1) or stimulated with 2 µM thapsigargin to deplete internal Ca^{2+} stores (TG; lane 3) or the vehicle control (DMSO; lane 2). Untreated cells (lane 1) were lysed, and the whole-cell lysate was analyzed by Western blotting using anti-STIM1 antibody. Cells treated with DMSO or TG were processed to determine PM-resident STIM1 (PM-STIM1) 30 s after the addition of DMSO or TG. Cell surface proteins were biotinylated, extracted with streptavidin-coated agarose beads, and analyzed by SDS-PAGE and Western blotting using the anti-STIM1 antibody. Positions of molecular mass markers are shown on the right of the blots. Data summary is shown in C and is representative of eight (eYFP-STIM1) and six (untagged STIM1) independent experiments.

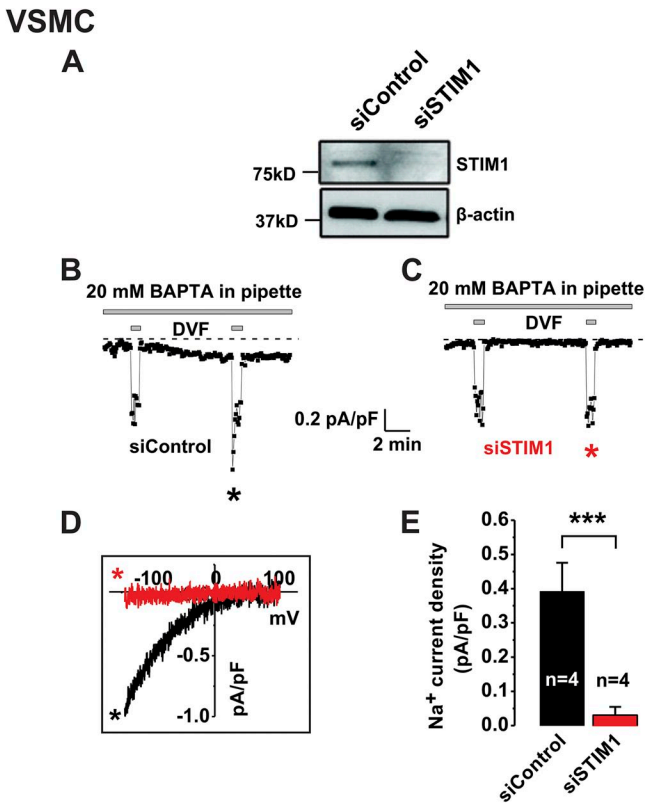

Figure S9. STIM1 knockdown abolished Na^+/Ca^{2+} currents in VSMCs. (A) Western blot in VSMCs showing that siRNA targeting STIM1 (siSTIM1) significantly down-regulated STIM1 protein expression. Whole-cell electrophysiological recordings on these VSMCs (C) show that STIM1 knockdown abolished Na^+/Ca^{2+} CRAC currents as compared with control (B). Representative Na^+ I-V relationships of CRAC currents in VSMCs are shown in D, and statistical analysis on current densities of Na^+ CRAC currents from each condition is shown in E.

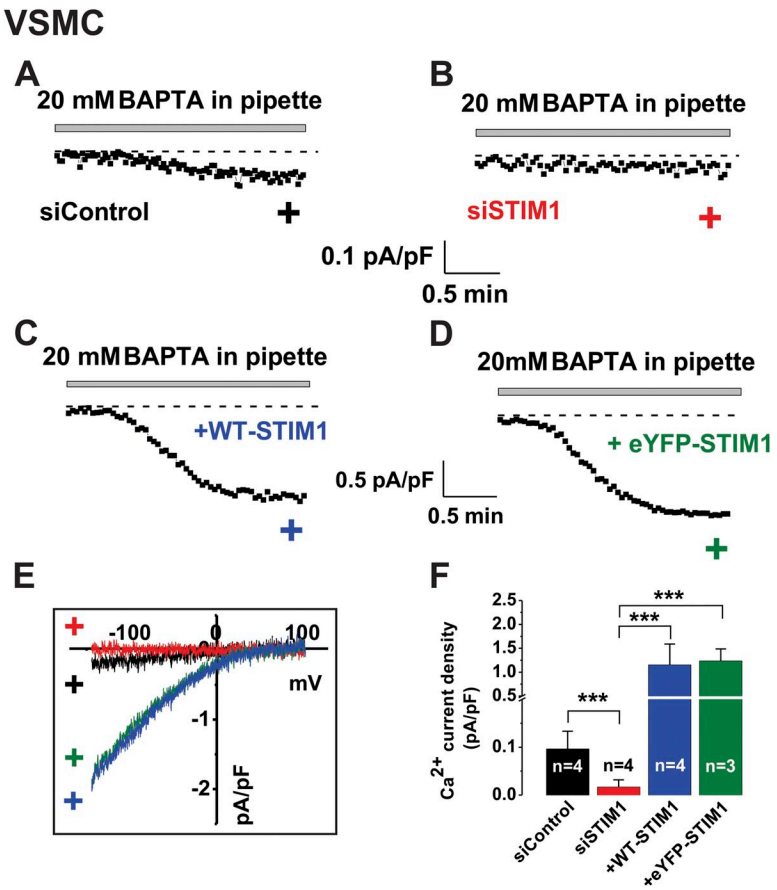

Figure S10. Both WT-STIM1 and eYFP-STIM1 rescued CRAC currents on STIM1 knockdown in VSMCs. Whole-cell patch-clamp recordings on VSMCs transfected with specific siRNA against STIM1 (siSTIM1) or siControl, a nontargeting control. STIM1 knockdown abrogated CRAC currents (B) as compared with control (A). Upon ectopic expression of plasmids encoding either WT-STIM1 (C) or eYFP-STIM1 (D) after STIM1 knockdown in VSMCs, both WT-STIM1 and eYFP-STIM1 rescued CRAC currents. Representative I-V curves taken from time course traces (A–D) where indicated by the color-coded "+" signs are shown in E. Statistical analyses on Ca^{2+} CRAC current densities for the four conditions in VSMCs (A–D) are shown in F. Please note that the scale for C and D is fivefold bigger than the scale for A and B.

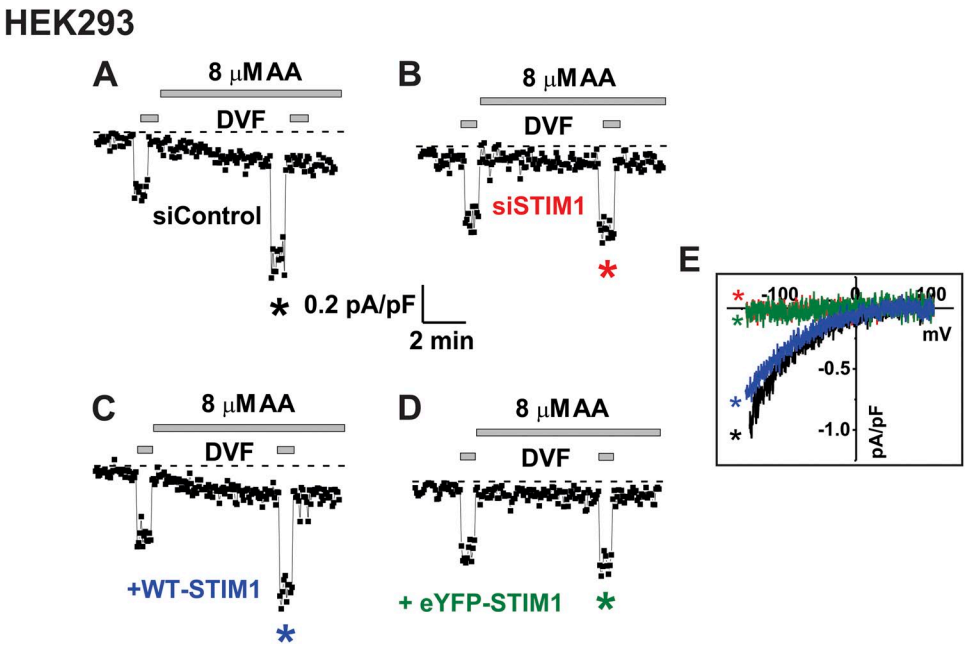

Figure S11. WT-STIM1 rescued AA-activated currents on STIM1 knockdown in HEK293 cells. Whole-cell patch-clamp electrophysiological recordings on HEK293 cells transfected with specific siRNA against STIM1 (siSTIM1; B) or siControl, a nontargeting control siRNA (A). STIM1 knockdown abrogated AA-activated currents (B) as compared with control (A). Upon ectopic expression of plasmids encoding either WT-STIM1 (C) or eYFP-STIM1 (D) after STIM1 knockdown in HEK293 cells, only WT-STIM1 rescued AA-activated currents. Representative I-V curves taken from time course traces (A–D) where indicated by the color-coded asterisks are shown in E. Statistical analyses on AA-activated current densities for the four conditions in HEK293 cells (A–D) are shown in Fig. 5 F in the main text.

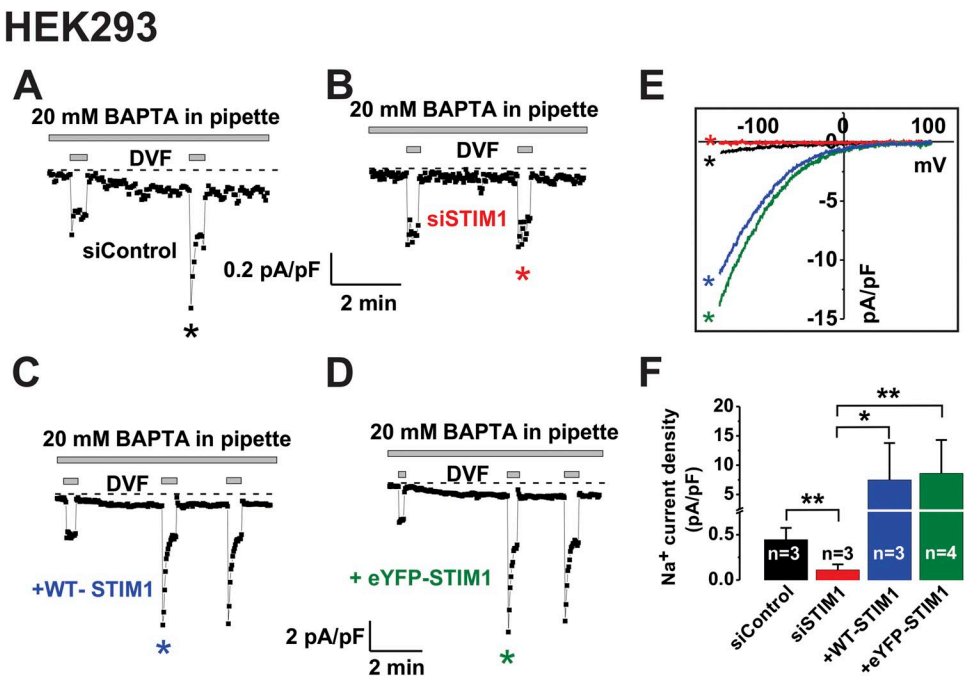

Figure S12. Both WT-STIM1 and eYFP-STIM1 rescued CRAC currents on STIM1 knockdown in HEK293 cells. Whole-cell patch-clamp recordings on HEK293 cells transfected with specific siRNA against STIM1 (siSTIM1) or siControl, a nontargeting control siRNA. STIM1 knockdown abrogated Na^+/Ca^{2+} CRAC currents (B) as compared with control (A). Upon ectopic expression of plasmids encoding either WT-STIM1 (C) or eYFP-STIM1 (D) after STIM1 knockdown in HEK293 cells, both WT-STIM1 and eYFP-STIM1 rescued CRAC currents. Representative I-V curves taken from time course traces (A–D) where indicated by the color-coded asterisks are shown in E. Statistical analyses on Na^+ CRAC current densities for the four conditions in HEK293 cells (A–D) are shown in F. Please note that the scale for C and D is 10-fold bigger than the scale for A and B.

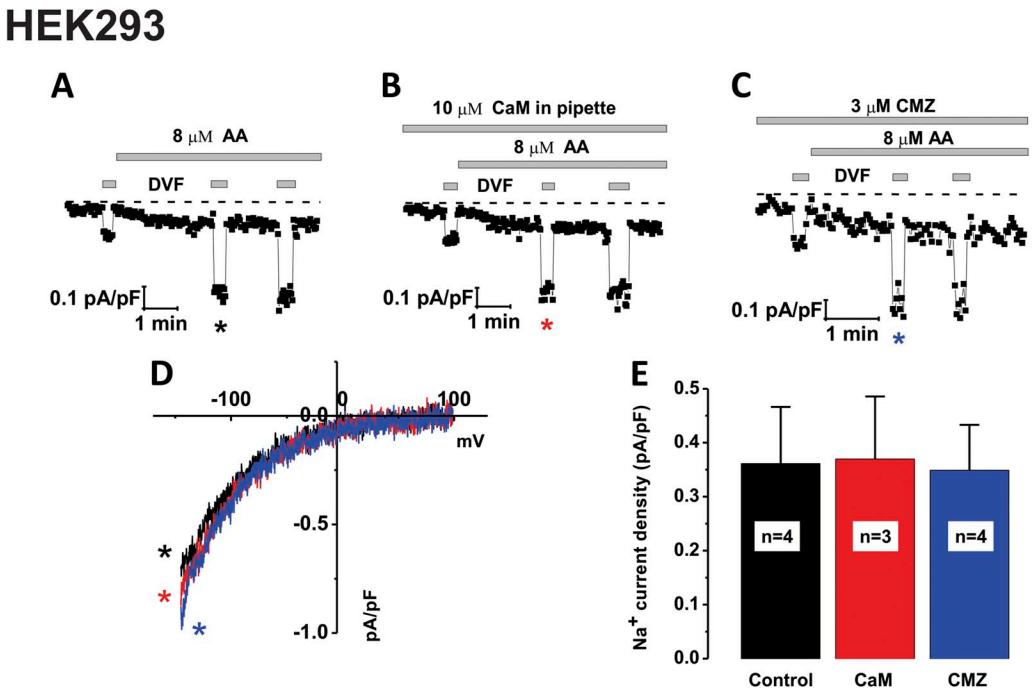

Figure S13. Calmodulin dialysis through the pipette and the addition of calmidazolium to the bath have no effect on AA-activated currents in HEK293 cells. Whole-cell patch-clamp electrophysiological recording on HEK293 cells. Dialyzing the cells with 10 μM calmodulin through patch pipette (B) or pretreatment of cells with 3 μM calmidazolium in the bath (C) has no effect on AA-activated currents as compared with control (A). Representative I-V curves are shown in D. Na^+ current densities measured under DVF bath solutions from three independent experiments are summarized in E.

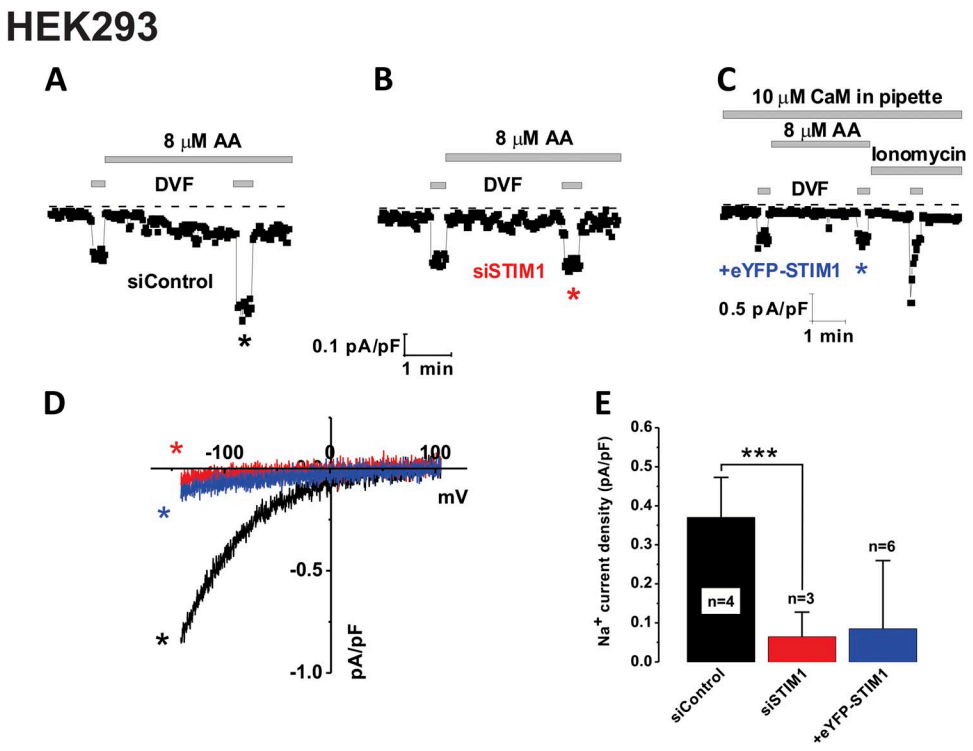

Figure S14. Combined calmodulin dialysis and eYFP-STIM1 expression in STIM1-depleted HEK293 cells failed to rescue AA-activated currents. Whole-cell patch-clamp electrophysiological recording on HEK293 cells transfected with specific siRNA against STIM1, or si-Control as a nontargeting control. STIM1 knockdown (B) completely abrogated AA-activated currents as compared with control (A). The combination of eYFP-STIM1 expression and 10 μM calmodulin dialysis through the patch pipette failed to rescue AA-activated currents in STIM1-depleted cells (C); the subsequent addition of ionomycin as a control showed that CRAC currents are rescued. Representative I-V curves are shown in D. Na^+ current densities measured under DVF bath solutions from three independent experiments are summarized in E.

Table S1
List of siRNA and shRNA sequences used in this study

siRNA/shRNA	Sequence
VSMCs (rat)	
siControl	UGGUUUACAUGUCGACUAA
siOrai2	GCCACAACCGUGAGAUCGA
siSTIM1	UAAGGGAAGACCUCAAUU
HEK293 cells (human)	
siControl	UGGUUUACAUGUCGACUAAUU
siOrai1	CGUGCACAAUCUCAACUCGUU
siOrai2	GGGCAUGGAUUACCGGGACUU
siOrai3	GGGUCAAGUUUGUGCCCAU
siSTIM1	AAGGGAAGACCUCAAUUACCAUU
VSMCs (rat)	
shControl	Open Biosystems sequence 1
shOrai1	GACCGACAGTTCCAGGAGCTCAACGAGCT
shOrai3	CCTCCCTTAGTTTAGCTTCTAA

Table S2
List of primers used for qPCR

Rat gene	Forward (5′–3′)	Reverse (3′–5′)	Size
			bp
rOrai1	ACGTCCACAACCTCAACTCC	ACTGTCGGTCCGTCTTATGG	362
rOrai2	CACCTATTTGCCCTGCTCAT	AGCTTGTGCAGTTCCTCGAT	386
rOrai3	CTGTCCACCAGTCACCACAC	CCACCAAGGATCGGTAGAAA	422

Table S3

Statistical analysis of patch-clamp data from supplemental figures

Figure	Cell type	Experiment	Stimulus	I[Ca^{2+}] (pA/pF)	*n*	I[Na^{+}] (pA/pF)	*n*	P-value
S1 C	VSMC	WT	None	0.008/0.012	4	ND	ND	
	VSMC	WT	AA	0.100/0.040	8	ND	ND	AA vs. Control; P = 4.14 E-07
S4 D	VSMC	shControl	BAPTA	ND	ND	0.391/0.042	4	
	VSMC	shOrai1	BAPTA	ND	ND	0.033/0.018	4	shOrai1 vs. shControl; P = 4.66 E-08
S4 H	HEK293	siControl	BAPTA	ND	ND	0.470/0.137	3	
	HEK293	siOrai1	BAPTA	ND	ND	0.131/0.105	4	siOrai1 vs. siControl; P = 5.86 E-04
S5 D	VSMC	siControl	BAPTA	ND	ND	0.411/0.072	3	
	VSMC	siOrai2	BAPTA	ND	ND	0.393/0.045	5	siOrai2 vs. siControl; P = 0.371
S5 H	HEK293	siControl	BAPTA	ND	ND	0.410/0.093	4	
	HEK293	siOrai2	BAPTA	ND	ND	0.396/0.068	5	siOrai2 vs. siControl; P = 0.552
S6 D	VSMC	shControl	BAPTA	ND	ND	0.398/0.064	3	
	VSMC	shOrai3	BAPTA	ND	ND	0.385/0.091	4	shOrai3 vs. shControl; P = 0.653
S6 H	HEK293	siControl	BAPTA	ND	ND	0.427/0.103	4	
	HEK293	siOrai3	BAPTA	ND	ND	0.446/0.121	4	siOrai3 vs. siControl; P = 0.591
S9 E	VSMC	siControl	BAPTA	ND	ND	0.392/0.084	4	
	VSMC	siSTIM1	BAPTA	ND	ND	0.031/0.024	4	siSTIM1 vs. siControl; P = 1.80 E-06
S10F	VSMC	siControl	BAPTA	0.097/0.037	4	ND	ND	
	VSMC	siSTIM1	BAPTA	0.017/0.015	4	ND	ND	siSTIM1 vs. siControl; P = 4.33 E-08
	VSMC	+WT-STIM1	BAPTA	1.153/0.436	4	ND	ND	+WT-STIM1 vs. siSTIM1; P = 6.25 E-06
	VSMC	+eYFP-STIM1	BAPTA	1.236/0.251	3	ND	ND	+eYFP-STIM1 vs. siSTIM1; P = 5.14 E-05
S12 F	HEK293	siControl	BAPTA	ND	ND	0.445/0.131	3	
	HEK293	siSTIM1	BAPTA	ND	ND	0.111/0.062	3	siSTIM1 vs. siControl; P = 0.00192
	HEK293	+WT-STIM1	BAPTA	ND	ND	7.467/6.304	3	+WT-STIM1 vs. siSTIM1; P = 0.0156
	HEK293	+eYFP-STIM1	BAPTA	ND	ND	8.592/5.701	4	+eYFP-STIM1 vs. siSTIM1; P = 0.00415
S13 E	HEK293	WT	AA	ND	ND	0.361/0.105	4	
	HEK293	WT	CaM + AA	ND	ND	0.349/0.084	3	CaM + AA vs. AA; P = 0.69439
	HEK293	WT	CMZ + AA	ND	ND	0.370/0.116	4	CMZ + AA vs. AA; P = 0.60203
S14 E	HEK293	siControl	AA	ND	ND	0.370/0.103	4	
	HEK293	siSTIM1	AA	ND	ND	0.064/0.063	3	siSTIM1 vs. siControl; P = 1.63 E-04
	HEK293	+eYFP-STIM1	CaM + AA	ND	ND	0.085/0.175	6	+eYFP-STIM1 vs. siSTIM1; P = 0.63144

Statistical analysis on patch-clamp experiments reported in the supplemental material, figure by figure, showing mean/range of Ca^{2+}/Na^{+} currents and corresponding *n* number and p-values for comparisons. WT, wild type; BAPTA, 1,2-bis(o-aminophenoxy)ethane-*N,N,N′,N′*-tetraacetic acid; AA, arachidonic acid; CMZ, calmadozolium; ND, not determined.